

Supporting Information For:

Role of Electron-Phonon Coupling in the Thermal Evolution of Bulk Rashba-Like Spin-Split Lead Halide Perovskites Exhibiting Dual-Band Photoluminescence

Julian A. Steele*,¹ Pascal Puech,² Bartomeu Monserrat,³ Bo Wu,⁴ Ruo Xi Yang,⁵ Thomas Kirchartz,^{6,7} Haifeng Yuan,⁸ Guillaume Fleury,¹ David Giovanni,⁹ Eduard Fron,⁸ Masoumeh Keshavarz,⁸ Elke Debroye,⁸ Guofu Zhou,⁴ Tze Chien Sum,⁹ Aron Walsh,^{10,11} Johan Hofkens,⁸ and Maarten B. J. Roeffaers*¹

1) cMACS, Department of Microbial and Molecular Systems, KU Leuven, Celestijnenlaan 200F, 3001 Leuven, Belgium

2) CEMES/CNRS, Université de Toulouse, 29, rue Jeanne Marvig, 31055 Toulouse, France

3) TCM Group, Cavendish Laboratory, University of Cambridge, J. J. Thomson Avenue, Cambridge CB3 0HE, United Kingdom

4) Guangdong Provincial Key Laboratory of Optical Information Materials and Technology & Institute of Electronic Paper Displays, South China Academy of Advanced Optoelectronics, South China Normal University, Guangzhou 510006, People's Republic of China

5) Molecular Foundry, Lawrence Berkeley National Laboratory, 1 Cyclotron Road, Berkeley, CA, United States

6) IEK5-Photovoltaics, Forschungszentrum Jülich, 52425 Jülich, Germany

7) Faculty of Engineering and CENIDE, University of Duisburg-Essen, Carl-Benz-Straße 199, 47057 Duisburg, Germany

8) Department of Chemistry, KU Leuven, Celestijnenlaan 200F, 3001 Leuven, Belgium

9) Division of Physics and Applied Physics, School of Physical and Mathematical Sciences, Nanyang Technological University, 21 Nanyang Link, Singapore, 637371, Singapore

10) Department of Materials, Imperial College London, Exhibition Road, London SW7 2AZ, United Kingdom

11) Global E3 Institute and Department of Materials Science and Engineering, Yonsei University, Seoul 120-749, Korea

Email: julian.steele@kuleuven.be, maarten.roeffaers@kuleuven.be

Methods

Materials:

CsPbBr₃ single crystal growth: Cesium bromide (CsBr), lead bromide (PbBr₂), dimethylformamide (DMF), acetonitrile (ACN), dimethyl sulfoxide (DMSO) ($\geq 99.9\%$), and γ -butyrolactone (GBL) ($\geq 99\%$) were purchased from Sigma-Aldrich. CsPbBr₃ SCs were prepared with a modified method from literature¹. Sub-mm sized CsPbBr₃ seeds were first prepared by heating an over-saturated precursor solution (with equal molar amounts of PbBr₂ and CsBr solids at the bottom of a 20 mL glass vial) on a hotplate at 75 °C. Small crystals attaching to the sidewall of the glass vial can be collected after 48 h. Right after collection with tweezers, several seeds were positioned into the growth solution for further growth. Briefly, methanol was added dropwise into a 0.45 M CsBr and PbBr₂ precursor DMSO solution at room temperature until a saturated precursor solution was achieved. The resulting solution was then filtered with a PTFE filter (0.2 μm). Several seeds were then added to the filtered growth solution. The growth solution with seeds was immediately positioned onto a hotplate at 30 °C for another 48 h. All crystals were washed with an excess amount of ACN after collection. After drying the crystals with Kimwipes, they were finally annealed at 50 °C for 5 min to remove any residual solvent on the crystal surface. The crystals have a typical dimension of 2–3 mm \times 2–3 mm \times 0.5–1 mm.

MAPbBr₃ single crystal growth: MAPbBr₃ SCs were prepared using the previously reported methods¹, via the inverse temperature crystallization method². For this, 1 M perovskite precursor solution of MAPbBr₃ in DMF were kept at 75 °C on a hotplate for several hours to allow SCs to form and grow, before they were selected and isolated.

Photoluminescence studies:

PL measurements were conducted by directing the excitation laser pulses to SCs. The laser pulses were generated by a 1-kHz regenerative amplifier (Coherent Libra, 800 nm, 50 fs, 4 mJ). A mode-locked Ti-sapphire oscillator (Coherent Vitesse, 80 MHz) was used for the amplifier. For 800 nm pump, the laser from the regenerative amplifier was directly used. For 400 nm, a BBO crystal was used to double the frequency of 800 nm. The photoluminescence was collected at a backscattering angle by a spectrometer (Acton, Spectra Pro 2500i) and CCD (Princeton Instruments, Pixis 400B). For circular-polarized pump and circular-polarized PL measurements, a quarter-waveplate and polarizer were placed in the path of the excitation beam and another pair of quarter-waveplate and polarizer were placed at the PL detection path.

Powdered X-Ray Diffraction (PXRD): PXRD patterns were recorded on a Malvern PANalytical Empyrean diffractometer ($\text{Cu K}_{\alpha 1} = 1.540598 \text{ \AA}$, $\text{K}_{\alpha 2} = 1.544426 \text{ \AA}$) in a high-throughput configuration using a PIXcel3D-Medipix3 1x1 detector.

Raman scattering spectroscopy:

Raman measurements using 808 nm excitation were carried out using a XY-Dilor spectrometer associated with a Ti-Sapphire (Ti: Al₂O₃) tunable laser which was pumped by an Argon laser. At this wavelength, the sample is transparent and no heating effect has been observed. We have used a long working distance $\times 40$ objective with a numerical aperture of 0.4 and selected a laser power under objective of 7 mW. A Princeton Instruments (PI) micro-cryostat able to monitor the sample temperature in the 80–300 K range has been used.

Raman experiments using 785 nm excitation were carried out using a MonoVista CRS+ Raman microscope (S&I). The laser was coupled into a microscope body (BX53F2, Olympus) equipped with an 10X 0.4 NA objective (UPlanSApo, Olympus). The

backscattered light is passed through a spectrometer (TriVista, Princeton Instruments) before reaching an electrically cooled EMCCD (Newton, Andor). The perovskite crystal was placed on a #1 glass coverslip inside a heating and freezing microscopy stage (HFS600, Linkam) connected to a Dewar filled with liquid nitrogen (DF2, Linkam) and a temperature controller. The sample was cooled between 300 K and 77 K at a rate of 20C/min with a dwell time of 10 min before the acquisition of spectra. For each measurement, an exposure time of 0.5 s and six accumulations were used.

DFT Calculations:

The orthorhombic structure of CsPbBr₃ was optimized by density functional theory (DFT) as implemented in the package VASP^{3,4}, with the functional PBEsol.^{5,6} In order to calculate the Raman spectrum of CsPbBr₃, the Gamma-point phonons were calculated using density functional perturbation theory as implemented in package VASP. We chose well-converged energy cutoff of 800 eV and k-point mesh of 10×10×8. Based on the character table of point group D_{2h}, we chose the Raman active phonon modes A_g, B_{1g}, B_{2g}, B_{3g} to generate the displaced structure and calculate the associated dielectric constants. Then the Raman peaks were simulated using the open-source package Phonopy-Spectroscopy.⁷

Supporting Data

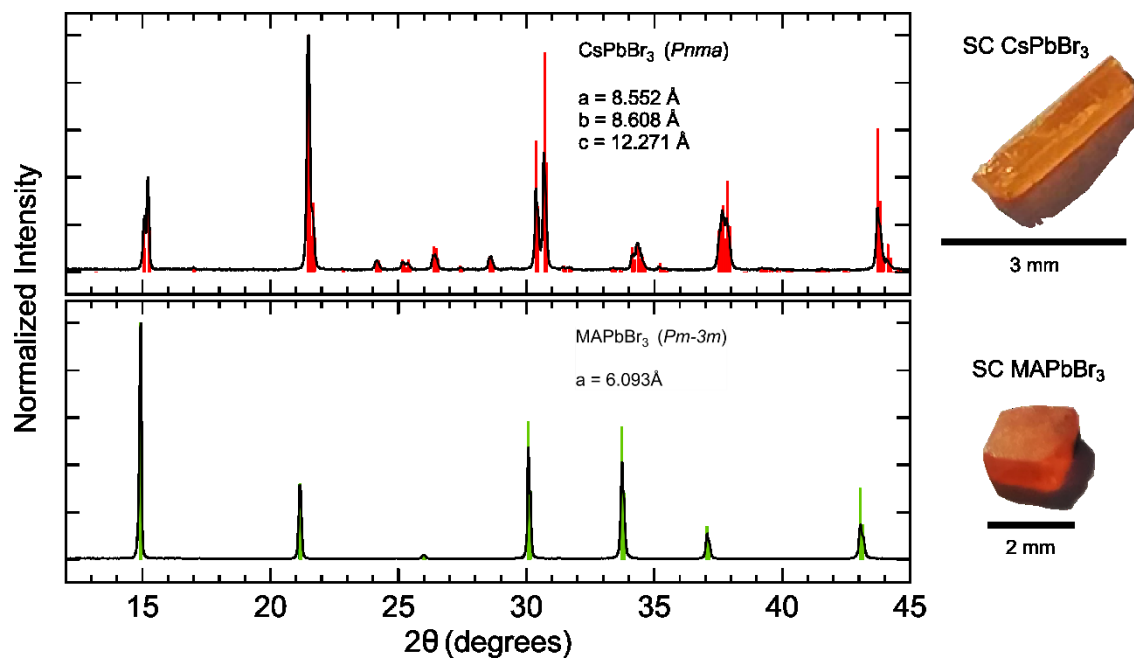


Figure S1: Left: Powdered X-ray diffraction scans of CsPbBr₃ and MAPbBr₃ mm-sized single crystals at RT, along with the simulated peaks (vertical colored sticks; VESTA software package) for the inset structure. Right: Images of typical crystal sizes and shapes of the respective perovskite materials.

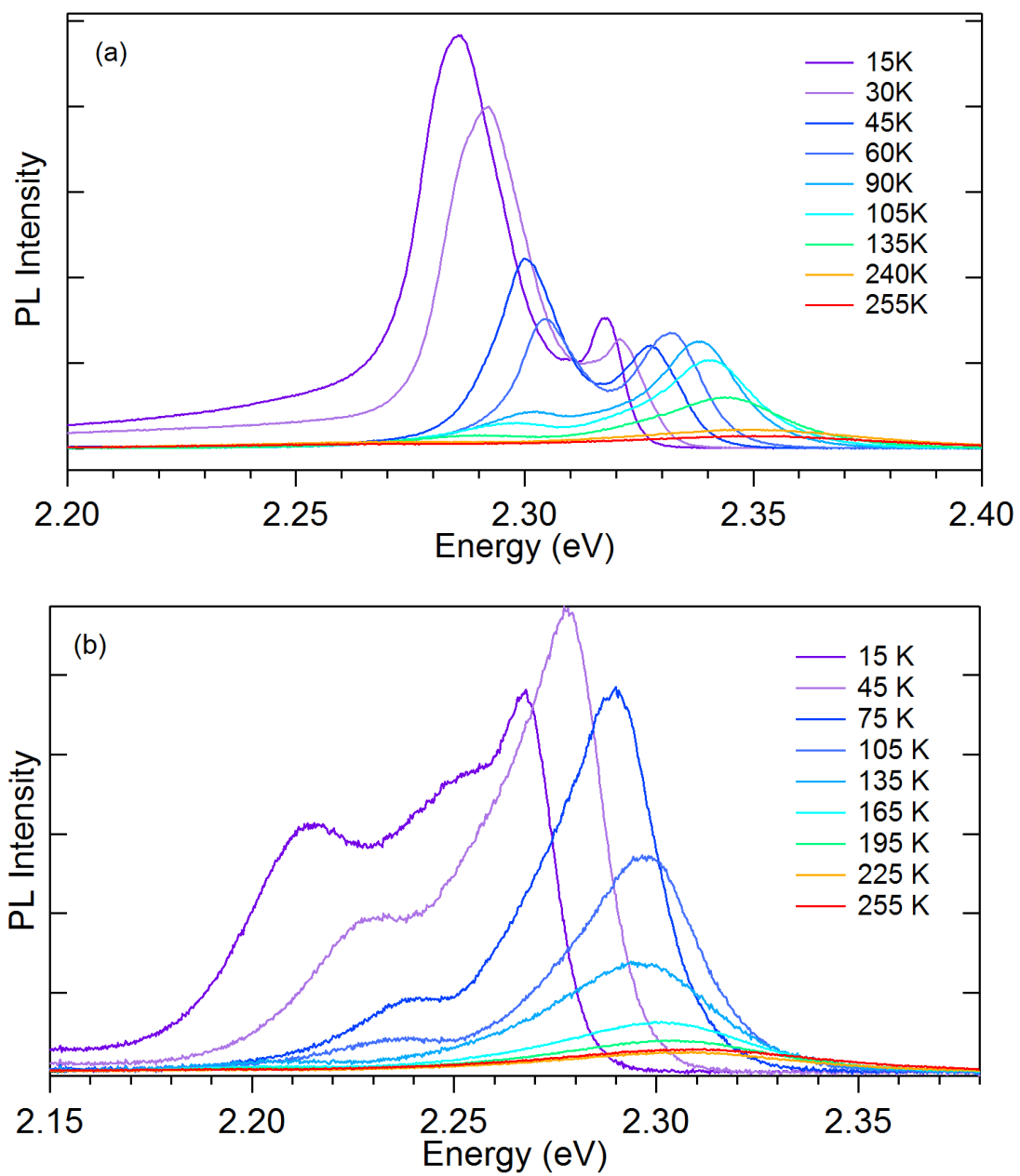


Figure S2: Non-normalized temperature-dependent PL spectra of (a) CsPbBr₃ and (b) MAPbBr₃.

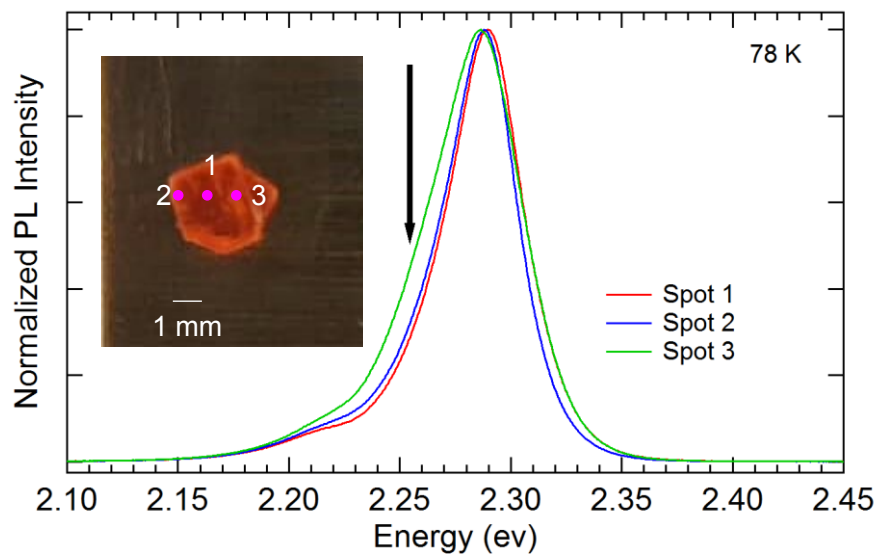


Figure S3: Comparison of normalized PL spectra (78 K) recorded from different locations on the SC MAPbBr₃ surface, which are shown in the inset optical image. The black arrow highlights the location-dependent asymmetric shoulder of the HE peak.

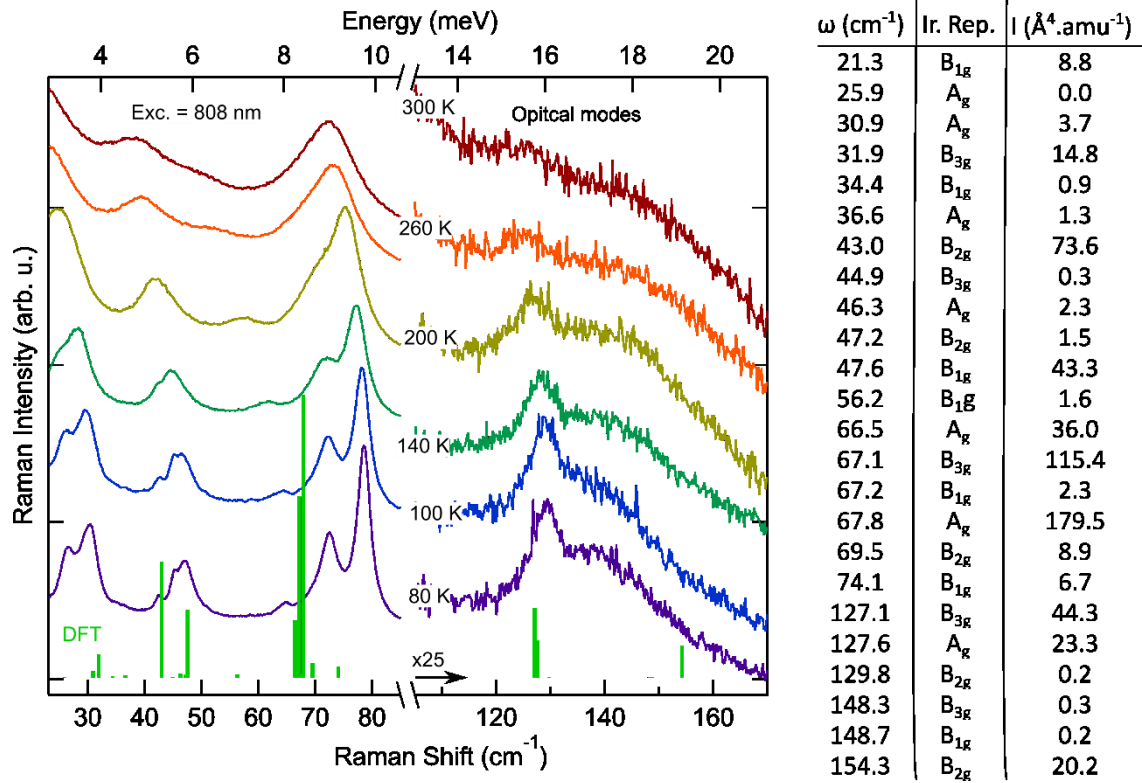


Figure S4: Temperature-dependent first order Raman scattering spectra of CsPbBr₃, highlighting the steady evolution of the high-energy optical modes (~17 meV) down to 80 K. The DFT determination of the frequency (ω), irreducible representation (Ir. Rep.) and Intensity (I) of the Raman active vibrations are provided on the right.

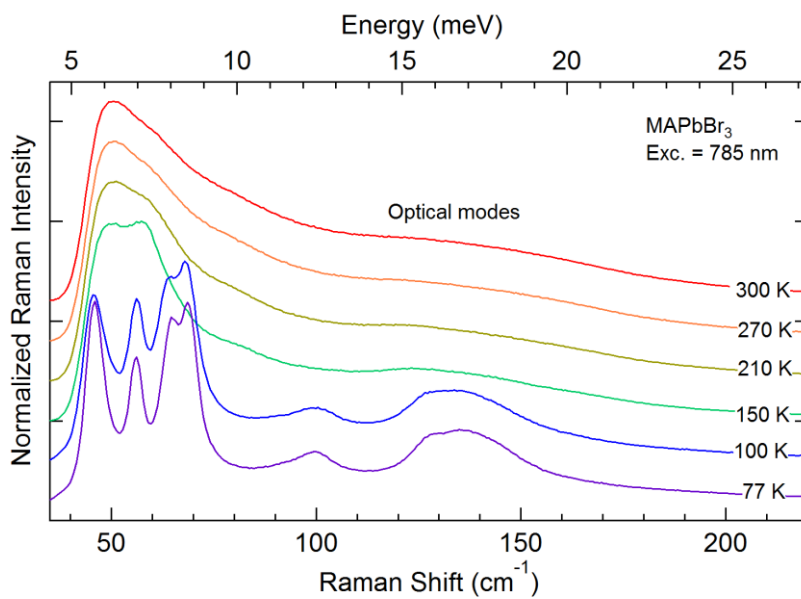


Figure S5: Temperature-dependent first order Raman scattering spectra of MAPbBr₃, highlighting the stable evolution of the high-energy optical modes (~17 meV) down to 77 K.

Table S1: Fitting parameter obtained by fitting the temperature dependence of the LE and HE peak energies with Equation 3 in the main text.

Peak	E_0 (meV)	A_1 (meV)	$\hbar\omega_1$ (meV)	A_2 (meV)	$\hbar\omega_2$ (meV)	A_3 (meV)	$\hbar\omega_3$ (meV)
LE (CsPbBr ₃)	2.287	106	3.8	-174	7.0	-186	14.7
HE (CsPbBr ₃)	2.316	106	3.8	-174	7.0	NA	NA
LE (MAPbBr ₃)	2.214	111	3.6	-191	6.4	-112	11.3
HE (MAPbBr ₃)	2.267	111	3.6	-191	6.4	NA	NA

Table S2: Fitting parameter obtained by fitting the temperature dependence of the LE and HE intensities with Arrhenius equations, taking into account one (LE) and two (HE) non-radiative channels.

Peak	I_0	a_1	E_{a1} (meV)	a_2	E_{a2} (meV)
LE (CsPbBr ₃)	0.995	29.9	10.9	NA	NA
HE (CsPbBr ₃)	0.0804	3.49	19.8	-2.035	6.6
LE (MAPbBr ₃)	0.35	19.0	18.1	NA	NA
HE (MAPbBr ₃)	0.698	16.4	42.5	-2.655	2.6

References:

1. Eperon, G. E. *et al.* Formamidinium lead trihalide: a broadly tunable perovskite for efficient planar heterojunction solar cells. *Energy & Environmental Science* **7**, 982 (2014).
2. Saidaminov, M. I. *et al.* High-quality bulk hybrid perovskite single crystals within minutes by inverse temperature crystallization. *Nature Communications* **6**, ncomms8586 (2015).
3. Perdew, J. P. *et al.* Restoring the Density-Gradient Expansion for Exchange in Solids and Surfaces. *Physical Review Letters* **100**, 136406 (2008).
4. Perdew, J. P. *et al.* Erratum: Restoring the Density-Gradient Expansion for Exchange in Solids and Surfaces [Phys. Rev. Lett. **100**, 136406 (2008)]. *Phys. Rev. Lett.* **102**, 039902 (2009).
5. Kresse, G. & Furthmüller, J. Efficient iterative schemes for ab initio total-energy calculations using a plane-wave basis set. *Physical Review B - Condensed Matter and Materials Physics* **54**, 11169–11186 (1996).
6. Kresse, G. & Furthmüller, J. Efficiency of ab-initio total energy calculations for metals and semiconductors using a plane-wave basis set. *Computational Materials Science* **6**, 15–50 (1996).
7. Brivio, F. *et al.* Lattice dynamics and vibrational spectra of the orthorhombic, tetragonal, and cubic phases of methylammonium lead iodide. *Physical Review B* **92**, 144308 (2015).